Analytical model for the airborne sound pressure waveform radiated when an offshore steel pipe pile is driven with an impact hammer

Marshall V. HALL[1]

[1] Marshall Hall Acoustics, Australia

ABSTRACT

An analytical model has been developed for the airborne sound pressure waveform radiated when an offshore steel pipe pile is struck by a short hammer. The model is based on the coupled equations of motion for axial and radial vibration of a thin shell, and yields frequency-dependent phase velocity and attenuation of these vibrations. A harmonic solution is obtained for the radiated sound pressure, using Junger & Feit's "Transform formulation of the pressure field of cylindrical radiators". The model is applied to a measurement of a 10-tonne hammer with cushion driving a pile 91 cm in diameter and 38 m long, in water 17 m deep. The height of the pile face above the water surface is estimated to have decreased from approximately 15 to 3 m during its driving. SPL (Leq) is examined at the measurement range (15 m) and microphone height (1.5 m). The present model predicts SPL would have ranged between 104 and 109 dB re 20 µPa as the pile face descended. The measured SPL data had an average of 103 dB and a maximum of 111 dB re 20 µPa. Possible reasons for the smaller spread of the model predictions are discussed.

Keywords: Emission Stationary Noise Sources I-INCE Classification of Subjects Number: 12.2.3

1. INTRODUCTION

Impact pile-driving radiates loud regular pulses of airborne noise, and a substantial amount of data has been presented in the literature on the measured Sound Pressure Level (SPL, or Leq) of these pulses. For piles made of steel, SPL averaged over 35 ms, "SPL(35ms)", at a horizontal range of 15 m is often in the neighbourhood of 100 dB re 20 µPa, which is 10-20 dB below the pain threshold for a human listener. The quantity of descriptive measured data on noise from pile driving is large. Beginning with [1], there have been many reports that used finite-element methods (FEM) to model axial displacement for the purpose of predicting pile-driver performance, but these reports treated the pile as a solid rod and neglected radial vibration. Since the area of the face is negligible in relation to that of the wall, the major sound signals will originate from radial vibration of the pile wall. In spite of this, an analytical model for radial vibration based on solutions to the equations of motion does not appear to exist.

Following an impact on a steel pile, a pulse of radial vibration (a bulge) travels down the pile much faster than sound travels through air. The first arrival at a microphone below the pile face therefore originates from a point on the pile a little higher than the microphone. This arrival has been described as a Mach wave. The trailing signal will be due to multipaths from portions of the pile both above and below the originating point.

The objective of the present paper is to present results from an analytical model for the vibration of a cylindrical shell and the consequent SPL of the radiated sound. A harmonic solution is obtained for the radiated sound pressure, using Junger and Feit's "Transform formulation of the pressure field of cylindrical radiators" [2]. The value of such a model is that it allows the relative importance of the driving parameters to be readily estimated and, in suitable cases, can be used as a benchmark for FEM models.

2. DEVELOPMENTS IN THE SHELL VIBRATION MODEL

The model produces an analytical expression for the spectrum of the vibration of a finite pipe pile

---

[1] marshallhall@optushome.com.au

when struck axially by a short hammer. A hammer cushion may be present. The coupled equations of motion for azimuth-independent axial and radial vibration (u and w) of a thin shell are solved. "For the thin-walled assumption to be valid the vessel must have a wall thickness of no more than about one-tenth (often cited as one twentieth) of its radius. This allows for treating the wall as a surface" [3]. The model yields frequency-dependent phase velocity and attenuation (due to radiation) for axial and radial vibration, and produces a complete description of the shell vibration. The present model is an extension of the previous model [4], in that a pile of finite length and the consequent reflections are now treated, as is the effect of a cushion in the hammer. The present model builds on Equations (1) to (34) in [4], albeit with the following amendments and qualifications:

2.1   Initial velocity of the pile face

In the general hammer there is an anvil (impact block), a cushion, and a helmet (drive cap) between the ram and the pile. The cushion separates the motion of the ram and anvil above it, from that of the helmet below it. The ram and anvil are assumed to be incompressible, and to have a common velocity following impact (v_a) which is obtained from conservation of momentum:

$$v_a = v_{ram} M_{ram} / \left(M_{ram} + M_{anvil} \right)$$

where v_{ram} is the velocity of the ram just prior to impact. For the impact between the anvil, cushion and helmet, the equations of motion for the axial displacements of the anvil $\theta(t)$ and helmet $\psi(t)$ are:

$$\left(M_{ram} + M_{anvil} \right) \ddot{\theta} + K \left(\theta - \psi \right) = 0$$

$$\left(M_{cushion} + M_{helmet} \right) \ddot{\psi} + A \rho_s q_y \dot{\psi} + K \left(\psi - \theta \right) = 0$$

where K is the stiffness of the cushion (which may be complex to represent damping within the cushion). It is assumed here that (i) all hammer components remain in contact until after impact with the pile, and (ii) the cushion is the only compressible hammer component. Taking the Fourier Transforms (FT) of the preceding equations and solving the resulting simultaneous equations in $\Theta(\omega)$ = FT$\{\theta\}$ and $\Psi(\omega)$ = FT$\{\psi\}$ yields

$$\Psi(\omega) = v_a / i\omega \left(\Omega + i\omega + \Delta(\omega) \right)$$

where

$$\Delta(\omega) = i\omega \left[\left(M_{cushion} + M_{helmet} \right) / \left(M_{ram} + M_{anvil} \right) \right] - \omega^2 A Y / q_y K - i\omega^3 \left(M_{cushion} + M_{helmet} \right) / K$$

and

$$\Omega = A Y / q_y \left(M_{ram} + M_{anvil} \right)$$

The cushion has two effects here: introduction of the variable $\Delta(\omega)$ into the spectrum of the helmet motion, and separation of the total mass of the four hammer components into two pairs. The velocity of the helmet $\dot{\psi}(t)$ may be obtained by taking the inverse FT (IFT) of $i\omega\Psi(\omega)$. For the impact between the helmet and the elastic pile face, it is assumed they will have a common velocity following impact that is also obtained from conservation of momentum (assuming the helmet and pile have the same densities and longitudinal sound speeds).

The Coefficient of Restitution (COR) of a hammer cushion is sometimes reported. For two colliding objects, COR is the ratio of their relative speeds after and before the collision. Instead of saying that an anvil rebounds upward after colliding with a cushion, the present model assumes they do not separate, and COR is used instead as an indicator of damping within the cushion. This is done in the following manner: if a cushion surface's (vertical) vibration $\theta(t)$ is a decaying oscillation, then the ratio of a positive peak to the next negative peak is considered as equivalent to COR. Thus the ratio of a positive peak to the next positive peak (a complete cycle) will be COR^2. If an acoustic wave exhibits this ratio then the medium would have a logarithmic decrement of - ln (COR^2), and the corresponding loss factor for the medium would be $1/Q$ = -(2/π) ln COR. This is readily incorporated in the model since the imaginary part of an elastic modulus is its real part divided by Q.

2.2   Boundary condition at the pile face

Deriving a boundary condition on the axial displacement (u) at the pile face requires that the relation between $\partial u/\partial t$ and $\partial u/\partial z$ be known. It was assumed in [4] that the phase velocity of u would equal a frequency-independent q_h, from which it would follow that $\partial u/\partial t = -q_h \partial u/\partial z$). As will be discussed later, the phase velocity (V) varies with frequency, and in particular $V \to q_y$ as $f \to 0$ if the internal medium is a gas or vacuum, whereas $V \to q_h$ as $f \to \infty$ for any medium, where

$$q_y = \sqrt{Y/\rho_s} \ , q_h = q_y \Big/ \sqrt{1-\nu^2}$$

in which Y, ρ_s and ν are the Young modulus, density and Poisson ratio of the pile (steel) material. The assumption of a constant V is therefore an approximation, and further work will be required to obtain a more accurate model.

2.3   Boundary condition at the pile wall

In deriving an expression for the Specific Acoustic Impedance (SAI) at the pile wall in [4] it was assumed that the medium inside the pile was a vacuum. It is now assumed that the internal medium is the same as the external medium, and the SAI at the wall as it was expressed in [4] is now identified as the external SAI. The internal SAI is similar to the external SAI, except that a Bessel function replaces each Hankel function. The "net" SAI that plays a role in the subsequent analysis is the difference between them.

2.4   Radial vibration

A shallow water environment is considered. The water surface is assumed to be a perfect reflector of sound, and consequently sound radiated by the aerial portion of the pile will remain airborne, and sound radiated from the submerged portion of the pile will remain underwater. In spite of this, it is necessary to take account of the underwater environment, in order that the reflections from the pile toe will be modelled accurately.

The FT of radial displacement w_n (z,t) will be denoted by $W_n(z,\omega)$. If reflections from the pile toe were neglected then $W_1(z,\omega)$ would be a downward travelling wave. At the toe, this wave is reflected upward. The reflectivity will be less than unity, since some vibration will radiate from the toe into the seabed. The reflection will create an additional term in W_1. The upward reflection will travel to the pile face where it will be reflected back downward. This cyclical behaviour will recur, but with diminishing amplitude.

3.   SCENARIO

The model is applied here to an example of the driving of a steel pile by an impact hammer, as reported by [5]. The pile driving project was located in Hood Canal in Kitsap County, Washington USA, and ran from 2012 September 28 to 2013 January 19. Overall, nearly 300 piles were installed. Each pile was driven in two stages, the first using a vibratory hammer and the second using an impact hammer.

3.1   The pile and its environment

The elastic properties of the pile steel were not described in [5]. It will be assumed here that the density was the standard value for steel of 7800 kg/m^3 [6]. The Young Modulus of steel can range between 195 and 206 GPa [7], and the minimum of this range is used since it yields an easily remembered longitudinal wave speed (q_y) of 5000 m/s. The Poisson ratio (ν) can range between 0.25 and 0.33 [7], and will be set at 0.3. The longitudinal loss factor (1/Q) can range between {0.2 and 3}$\times 10^{-4}$ [6], and will be set to the maximum value (which corresponds to an absorption rate of 0.008 dB per wavelength). This loss factor has a negligible effect on the model, and is included only for illustrative purposes.

Airborne (and underwater) acoustic measurements were taken throughout the pile driving project described by [5]. From the data for many piles, one pile was selected for consideration on the basis that the noise was measured overwater at a convenient range of 15 m, and the pile length was given (38 m). Data at longer ranges were also reported, but were not selected owing to an expected increase in the uncertainty in propagation loss. The pile selected, named 'T22-B', had an external radius of 45.7 cm. The wall thickness was not stated, but has been estimated at 1.905 cm (4.2% of the radius) since this was the thickness of most piles with the same radius driven at the same location a year previously [8].

On January 7, prior to impact driving, the selected pile had been driven with a vibratory hammer for 330 seconds. Since the seafloor depth during the vibratory stage was reported as 20 m, the height of this pile's face at the beginning would have been 18 m. How far the pile penetrated into the seabed by the conclusion of the vibratory stage was not reported, but may be presumed to be several metres.

On January 19, the selected pile was driven with an impact hammer for 52 seconds, during which time there were 32 hammer blows [5]. Even with a comparatively large "set" (penetration per blow)

of say 0.3 m, the total descent of the pile would have been approximately 10 m. The seafloor depth during the impact driving of this pile was reported as 17 m. The impact driving would presumably have continued until the pile face height was suitable for the planned wharf. According to [9], in response to a submission on the same wharf as that addressed by [5], "The elevation of the top of the wharf deck will be 20.5 ft above MLLW, and the bottom of the wharf deck will be 13 ft above MLLW" (MLLW means 'Mean Lower Low Water, the datum used for reporting tide height in the local area). The height of the pile face at MLLW will therefore be taken as 20.5 ft, or 6.25 m. The driving of the selected pile was completed at 11:09 on 2013 January 19, at which time the tide height according to the NOAA tide calculator [10] was 3.25 m. The height of the pile face is therefore estimated to have decreased from approximately 15 to 3.0 m during the impact driving.

Since the air and water sound-speeds were not given in [5], they have been estimated on the basis of the low sea-surface temperature (8 C) where the measurements were taken [11]. The estimates obtained are $c_1 = 330$ and $c_2 = 1480$ m/s.

The seabed soil ranged from poorly graded gravel-silty gravel to silty sand/gravel [5], from which the seabed's mean grain-size was estimated to be 1 ϕ. The estimated seabed sound-speed is therefore given by $c_3 = 1.17\, c_2$, and the estimated seabed density by $\rho_3 = 2.1\, \rho_2$ [12].

3.2   The hammer

The impact and vibratory hammers used were manufactured by American Piledriving Equipment, Inc. (APE). For the impact driving, the hammer models were APE D-80 and APE D-100, each of which is a diesel hammer and contains a hammer cushion. According to the manufacturer of the Delmag diesel hammer [13], the role of the diesel fuel is as follows:

.. Injection of diesel fuel and compression. While dropping…a certain quantity of fuel is sprayed on top of the impact block. After passing the exhaust ports, the piston starts compressing the air in the combustion chamber. Impact and Combustion. The impact of the piston on the impact block atomizes the diesel fuel in the combustion chamber. The atomized fuel ignites in the highly compressed air. The combustion energy moves the piston upwards… Three different energies are acting on the pile: Compression + Impact + Combustion.

On a schematic diagram of Force vs time [14], the force on the pile due to compression is not shown (so presumed to be small), the force due to impact has a sharp peak, and the force due to combustion has a broad peak with an amplitude that is around one-half of the impact peak. On this basis, it will be assumed here that the effect of combustion on radiated SPL will be negligible.

The hammer used to drive the selected pile was the D-100 model, whose ram has a mass of 10000 kg. The specifications [15] for this hammer indicate that it can operate with a driving kinetic energy of up to 335 kJ, for which the corresponding impact velocity is 8.19 m/s. The masses of the anvil and striker plate were 2118 and 470 kg respectively [15] and these are lumped together. The mass of the drive cap (helmet) is not given for the APE D100, but is given as 1104 kg for the APE D62 model, and this is assumed here to apply to the D100. This hammer has a cushion, which has a thickness of 8.89 cm, an Elastic (Young) modulus of 1965 MPa, and a COR of 0.8 [15]. From the dimensions given for the Aluminium and Micarta layers in the cushion, its total mass has been estimated as 53 kg.

4.   RESULTS FROM THE SHELL VIBRATION MODEL

4.1   Spectra of phase velocity and damping rate

The longitudinal phase velocity, Real (V), is shown in Figure 1 as a function of frequency up to 8 kHz. In medium 1 (air), $V_1 \to q_y$ as $f \to 0$. In the denser liquid media, this limit is somewhat higher. As f becomes large, $V_n \to q_h$ for all three media. The large swings at frequency near 1.8 kHz are associated with the expression for S, in which it can be seen that V will be large at $\omega = q_y/a$ and q_h/a unless the SAI are also large (as will occur in a liquid). For the case at hand (a = 0.457 m), the two corresponding "critical" frequencies are 1740 and 1820 Hz. The minimum value of V_1 (not shown) is 43 m/s at 1762 Hz, and the maximum is 54 km/s at 1826 Hz.

In medium 2, sharp minima and maxima occur at a spacing of 1.8 kHz at the higher frequencies. If there is no liquid in the pile interior, it was shown in [4] that V_2 increased rapidly from below q_y to above q_h as frequency increased past the critical frequencies, and then decreased monotonically to q_h as frequency continued to increase. The sharp extrema may therefore be attributed to the liquid internal medium, and in particular to resonances in the standing waves therein. There is also some variation in V_3 in the seabed, although less pronounced than for V_2 in water. This smaller effect is attributed to

the seabed being assigned an intrinsic absorption coefficient (of 1 dB /wavelength).
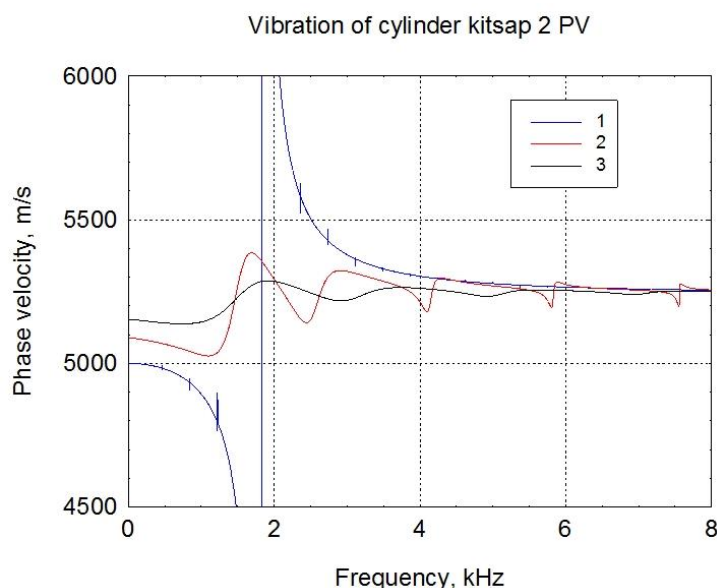
Vibration of cylinder kitsap 2 PV

Figure 1: Longitudinal phase velocity vs frequency along the steel pile selected from the data presented by [5] when surrounded by air (1), seawater (2) and seabed (3) respectively.

The longitudinal damping rate (DR) in decibels per wavelength is shown as a function of frequency in Figure 2. At a given frequency f, the wavelength is obtained from $\lambda = V /f$, and this λ is multiplied by the damping in dB per unit length [proportional to Imag (V)] to yield damping per wavelength. In air (medium 1), this DR equals the intrinsic damping in steel, except near and between the two critical frequencies. In the liquid media the SAI are large, and no particular behavior occurs near the critical frequencies. The extrema spaced 1.8 kHz apart at the higher frequencies are again evident.
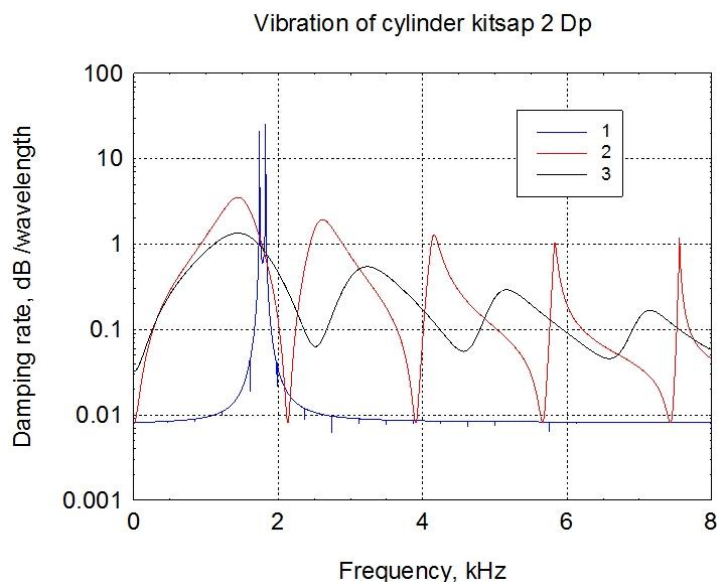
Vibration of cylinder kitsap 2 Dp

Figure 2: Longitudinal damping rate along the same pile whose phase velocity is presented in Figure 1.

4.2   Axial and radial vibrations of the pile wall

The FTs (spectra) of the pile wall's axial and radial velocities at the pile face (z = 4 m) and at the water surface (z = 0) are shown in Figure 3, computed for a COR of 0.8. A peak that is common to all four spectra occurs at approximately 410 Hz. This is attributed to the oscillation of the cushion, which has a resonance frequency (f_0) where the denominator in the expression for the spectrum for the

helmet's axial displacement (Ψ in the equations above) has its minimum. This will occur approximately where the imaginary part is zero (since the real part is never zero). Equating the sum of the two terms in the imaginary part to zero and solving for the resonance frequency yields $f_0 = 408$ Hz.

At the pile face the axial spectrum falls off monotonically with frequency (above 408 Hz), while at the water surface it has a deep sharp minimum in the band between the two critical frequencies (due to the high damping in that band). At frequencies outside the critical band, the two axial spectra are indistinguishable, due to the negligible damping in the aerial portion of the pile. The radial spectrum at the face has sharp peaks at the two critical frequencies, which at the surface transform into a deep minimum in the band between the critical frequencies.
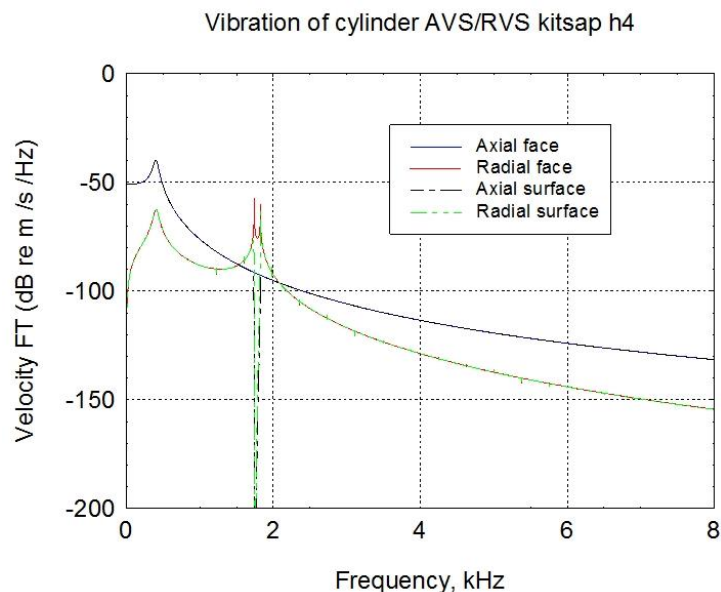

Figure 3: Fourier Transforms of the pile wall's axial and radial velocities at the pile face and water surface.

Each velocity waveform, which is the IFT of the corresponding spectrum, was computed with a frequency pixel of 0.49 Hz. For negative frequencies the (complex) FT was set to the conjugate of its value at the "mirror" positive frequency, and thus the resulting waveform should be real. With this frequency pixel, the shortfall in the energy in the real part of each waveform was generally less than 0.05 dB in comparison with the energy in the spectrum (the shortfall increased if the frequency pixel was increased). On this basis the real waveforms are regarded as accurate to within 0.05 dB. The waveform of the pile wall's axial velocity at the pile face is shown in Figure 4. The waveform at the water surface is not shown since it is very similar to that at the face; the main noticeable difference being that the waveform is delayed by around 1 ms.
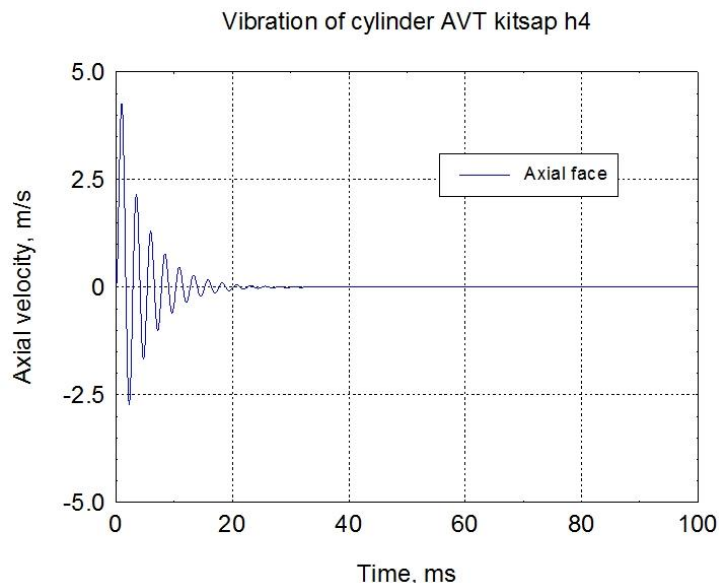
Vibration of cylinder AVT kitsap h4

Figure 4: Waveform of the pile wall's axial velocity at the pile face.

The waveforms of the radial velocity at the pile face and water surface are shown in Figure 5. It can be seen that the axial and radial velocities are both decaying sinusoidal oscillations with a frequency of around 410 Hz. The radial velocity is approximately 6% of the axial. Whereas the axial velocity is approximately the same at the two heights (apart from a 1-ms time delay), the radial velocity has reduced a little (particularly the later arrivals), due to the loss of the energy in the band between the critical frequencies. The reason for the (small) decrease in radial velocity from the face to the surface is that the aerial portion of the pile has radiated sound into the air.
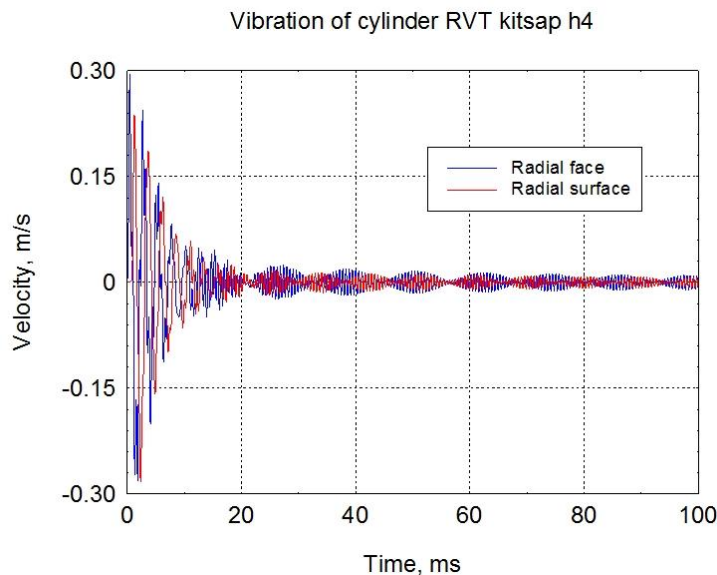
Vibration of cylinder RVT kitsap h4

Figure 5: Waveforms of the pile wall's radial velocity at the pile face and water surface.

5. RADIATED SOUND

5.1 Transform formulation of the pressure field of cylindrical radiators

The "Transform formulation of the pressure field of cylindrical radiators" [2] is applied to $W(z,\omega)$. The present model extends from the algorithm as implemented in [4] in two respects:

(i) Whereas [2] and [4] considered the surrounding medium to be unbounded, the present model modifies the algorithm to account for a surface (at $z = 0$) with a reflectivity of +1 for airborne sound.

The present model assumes however that a sound source below that surface will have no effect on a receiver above the surface.

(ii) Whereas [2] and [4] considered the surrounding medium to be homogeneous, the present model allows the value of V and DR on the pile to vary with height or depth in accordance with the properties of the surrounding medium.

5.2   Wavenumber (γ) Fourier Transform

The analysis in [2] used the vertical wavenumber (γ) FT of the height-dependence of radial vibration: F(γ) = FT{W(r,z,ω)}. F is a function of r and ω as well as γ, but these dependencies are suppressed for clarity. The frequency FT of the pressure waveform p(r,z,t), which will be denoted by P(r,z,ω), therefore includes a γ IFT of a function of γ that contains F(γ) as a factor.

When toe reflection is included, the expression for F(γ) is an infinite sum of down-going and up-going terms.

At each frequency selected for the IFT, which will be required in order to obtain p(r,z,t) from P(r,z,ω), the γ IFT needs to be computed by numerical integration. The method chosen here is the straightforward (but slow) IMSL routine "DQDAGS", which is an adaptive, general purpose routine for which endpoint singularities are acceptable. At each frequency, the integration intervals are defined as $[- 1.2 \, \omega/c_2, + 1.2 \, \omega/c_2]$. The stationary phase approximate method has been tried in an underwater environment [16], but found to give large errors. These errors occur because F(γ) has peaks, but for q > c the peaks are not points of stationary phase.

5.3   Sound pressure spectrum

A sound pressure spectrum P(r,z,ω) has been computed for range 15 m, face height 4 m, and receiver height 1.5 m. The magnitude of the result is shown in Figure 6. The peaks at around 400 Hz (cushion resonance) and 1800 Hz (pile radius resonance) are again evident. The spectrum energy, obtained from the frequency integral $\int |P(\omega)|^2 \, df$, is 92.52 dB re 20 μPa^2.s.
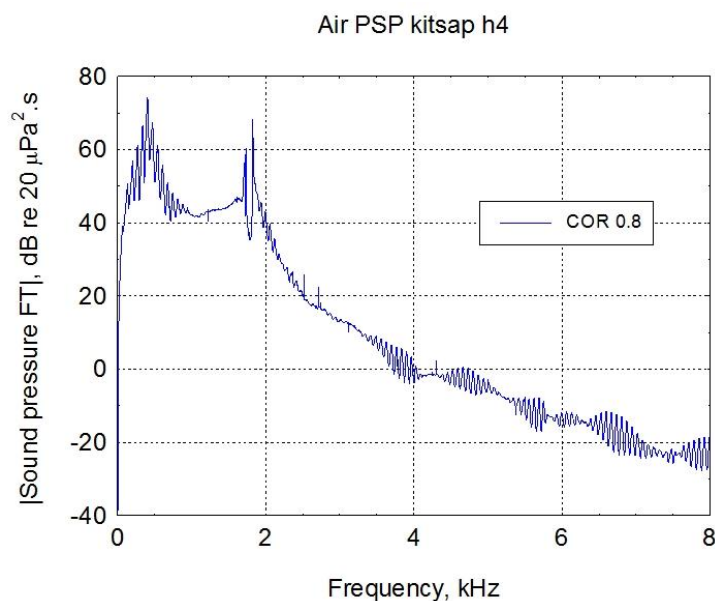

Figure 6: Fourier Transform of the radiated pressure at range of 15 m and receiver height 1.5 m.

5.4   Sound pressure waveform

A sound pressure waveform p(r,z,t) has also been computed for range 15 m, face height 4 m, and receiver height 1.5 m. The result, which is shown in Figure 7 out to 250 ms following impact, is the real part of a complex waveform produced using the same settings as for the shell vibration waveforms. The waveform energy, obtained from the time integral $\int p(t)^2 \, dt$, is 92.48 dB re 20 μPa^2.s (0.04 dB less than the frequency integral). The successive pulses at time delays of approximately 15 ms are reflections from the pile toe.
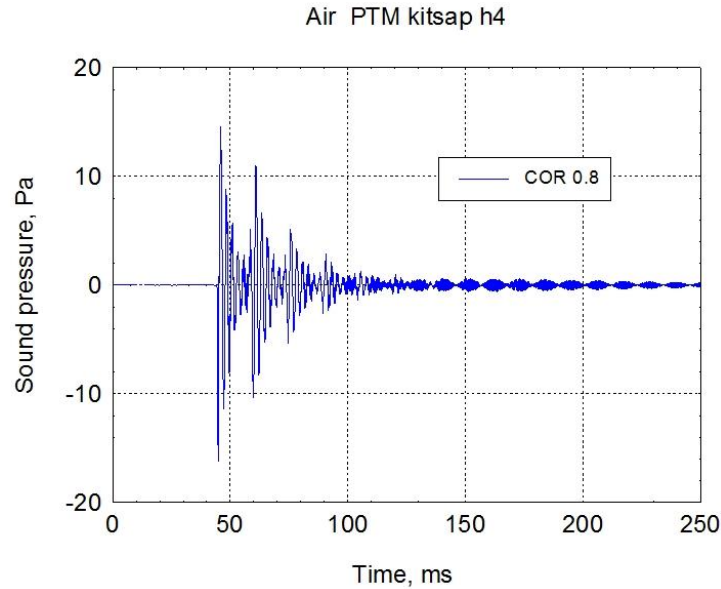
Air PTM kitsap h4

Figure 7: Radiated pressure waveform at range 15 m and height 1.5 m, out to 250 ms after impact.

5.5   Comparison with data

In analyzing the sound pressure waveform data from a single hammer blow, the analysts who contributed to [5] computed the RMS SPL of successive intervals of duration 35 ms, and noted the maximum value of these individual SPLs over the duration of the waveform. Referring to Figure 7 for example, and treating it as data, the second interval [35-70 ms] would yield the maximum SPL. Since the RMS pressure over that interval is 4.2 Pa, the corresponding SPL would be 20 log(4.2) + 94 = 106 dB re 20 µPa. For each pile, [5] reported the average and maximum of these results over the number of blows struck. For the selected pile, which was struck 32 times, the average and maximum SPL were reported as 103 and 111 dB re 20 µPa respectively. The maximum SPL(35 ms) predicted by the present model is shown in Figure 8 as a function of pile face height (from 3 to 15 m) for the nominal COR of 0.8. It can be seen that the average SPL as the pile descended would be approximately 107 dB re 20 µPa, while the maximum would be 109 dB re 20 µPa. The predicted average is 4 dB higher than the measured average, while the predicted maximum is 2 dB lower than the measured maximum.
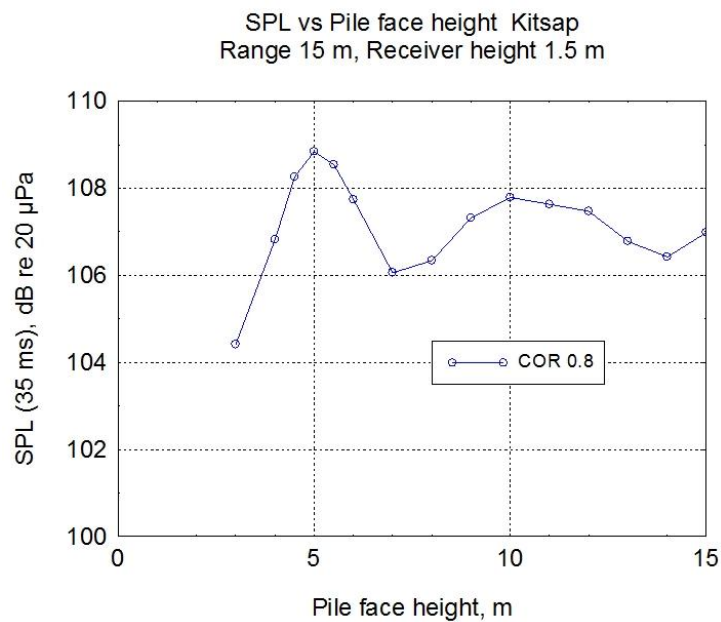
SPL vs Pile face height Kitsap
Range 15 m, Receiver height 1.5 m

Figure 8: Predicted SPL (35 ms) vs. pile face height for a Cushion Restitution Coefficient of 0.8

6. CONCLUSIONS

An analytical model has been developed for the airborne sound pressure waveform radiated when an offshore steel pipe pile is struck by a short hammer, and applied to a measurement of a hammer with cushion driving an offshore pile. The height of the pile face m above the water surface is estimated to have ranged between approximately 3 and 20 m. SPL (Leq) averaged over 35 ms at range 15 m is examined for a microphone height of 1.5 m. On the assumptions that the seabed was a uniform liquid (rather than becoming more solid with depth) and that the cushion's coefficient of restitution of 0.8 was due to damping within the cushion, the present model predicts SPL would have ranged between 104 and 108 dB re 20 µPa as the pile descended. The measured SPL data had a wider spread of values, with an average of 103 dB re 20 µPa and a maximum of 111 dB re 20 µPa. Possible reasons for the smaller spread of the model predictions are discussed

REFERENCES

1. Smith EAL. Pile driving analysis by the wave equation. J Soil Mech and Found ASCE. 1960; 86: 35-61.
2. Junger MC, Feit D. Sound, Structures, and Their Interaction. New York: Acoustical Society of America; 1993.
3. Anonymous. Cylinder Stress. Wikipedia http://en.wikipedia.org/wiki/Cylinder_stress. Retrieved 2014 Jul 16.
4. Hall MV. A semi-analytical model for non-Mach peak pressure of underwater acoustic pulses from offshore pile driving. Acoustics Australia. 2013; 41 (1): 42-51.
5. Navy Strategic Systems Programs. Naval Base Kitsap at Bangor, Trident Support Facilities Explosive Handling Wharf (EHW-2) Project, Acoustic Monitoring Report, Bangor, Washington. Prepared by Illingworth & Rodkin, Inc. 2013. Downloaded from www.nmfs.noaa.gov. Retrieved 2014 Aug 13.
6. Irvine T. Damping properties of materials Revision C. 2004.
   http://syont.files.wordpress.com/2007/05/damping-properties-of-materials.pdf. Retrieved 2014 Jul 16.
7. Yarwood TM, Castle F. Physical and mathematical tables. London: Macmillan & Co. Ltd; 1959.
8. NAVFAC. Naval Base Kitsap at Bangor EHW-1 Pile Replacement Project, Bangor, Washington. Final Acoustic Monitoring Report. Prepared by Illingworth & Rodkin, Inc. 2012. Downloaded from www.nmfs.noaa.gov. Retrieved 2014 Aug 13.
9. Berg KS. Second Explosives Handling Wharf at Naval Base Kitsap Bangor, Endangered Species Act Section 7 Formal Consultation. U.S. Fish and Wildlife Service 2011. Downloaded from www.fws.gov. Retrieved 2014 Aug 13.
10. NOAA Tides and Currents BANGOR, WA StationId: 9445133
    http://tidesandcurrents.noaa.gov/noaatidepredictions/NOAATidesFacade.jsp?Stationid=9445133
    Retrieved 2014 Aug 13
11. NOAA National Oceanographic Data Center (NODC). Water Temperature Table of the Northern Pacific Coast. http://www.nodc.noaa.gov/dsdt/cwtg/npac.html Retrieved 2014 Aug 13
12. Richardson MD, Briggs KB. On the use of acoustic impedance values to determine sediment properties. Proceedings of the Institute of Acoustics, UK. 1993; 15 (2): 15-24
13. Anonymous. DELMAG Pile Driving Equipment Technical data. Esslingen Germany: DELMAG GmbH + Co.KG; 2010. http://www.delmag.com/technical-data.html   Retrieved 2014 Jul 22.
14. Anonymous. DELMAG Pile driving equipment. Esslingen Germany: DELMAG GmbH + Co.KG; 2010. Downloaded from "DELMAG diesel pile hammers" www.delmag.com/diesel-pile-hammers.html Retrieved 2014 Aug 6
15. Anonymous. APE D100-42 Single Acting Diesel Impact Hammer. American Piledriving Equipment, Inc. www.apevibro.com/pdfs/diesels/specs/d100-42.pdf. Retrieved 2014 Aug 13.
16. Hall MV. Development of a semi-analytical model for the underwater radiated noise from a driven pile – comparison of the stationary phase approximation with exact integration for computing an inverse Fourier Transform of vertical wavenumber (A). J Acoust Soc Am. 2014; 135 (4): 2300.